

AperTO - Archivio Istituzionale Open Access dell'Università di Torino

A fluid inclusion study of blueschist-facies lithologies from the Indus suture zone, Ladakh (India): Implications for the exhumation of the subduction related Sapi-Shergol ophiolitic mélange

This is the author's manuscript

Original Citation:

Availability:

This version is available <http://hdl.handle.net/2318/1641102> since 2017-06-06T14:32:16Z

Published version:

DOI:10.1016/j.jseaes.2017.05.025

Terms of use:

Open Access

Anyone can freely access the full text of works made available as "Open Access". Works made available under a Creative Commons license can be used according to the terms and conditions of said license. Use of all other works requires consent of the right holder (author or publisher) if not exempted from copyright protection by the applicable law.

(Article begins on next page)

**A fluid inclusion study of blueschist-facies lithologies from the Indus suture zone,
Ladakh (India): Implications for the exhumation of the subduction related Sapi-Shergol
ophiolitic mélange**

By

Himanshu Kumar Sachan^{1*}, Aditya Kharya¹, P. Chandra Singh¹, Franco Rolfo², Chiara
Groppo², Sameer Tiwari¹

1 Wadia Institute of Himalayan Geology, 33 GMS Road, Dehra Dun – 248 001 (India)

2 Department of Earth Sciences, University of Torino, Via Valperga Caluso 35, Torino,
10125, Italy and IGG-CNR, Via Valperga Caluso 35, Torino, 10125, Italy

Corresponding author: *hksachan@wihg.res.in

Abstract

The best occurrence of blueschist-facies lithologies in Himalaya is that of the Shergol Ophiolitic Mélange along the Indus suture zone in Ladakh region of north-western India. These lithologies are characterized by well preserved lawsonite-glaucophane-garnet-quartz assemblages. This paper presents for the first time the results of a detailed fluid inclusion study on these lithologies, in order to understand the fluid P-T evolution and its tectonic implications.

The blueschist rocks from Shergol Ophiolitic Mélange record metamorphic peak conditions at ~ 19 kbar, 470°C. Several types of fluid inclusions are trapped in quartz and garnet, most of them being two-phase at room temperature. Three types of fluid inclusions have been recognised, basing on microtextures and fluid composition: Type-I are primary two-phase carbonic-aqueous fluid inclusions ($V_{CO_2} - L_{H_2O}$); Type-II are two-phase ($L_{H_2O} - V_{H_2O}$) aqueous fluid inclusions, either primary (Type-IIa) or secondary (Type-IIb); Type-III are re-equilibrated fluid inclusions. In the Type-I primary carbonic-aqueous inclusions, H_2O is strongly predominant with respect to CO_2 ; the homogenization temperature of CO_2 range from -7 to -2°C. The clathrate melting temperature in such inclusions varies in between +7.1 to +8.6°C. Type-II two-phase aqueous fluid inclusions show a wide range of salinity, from 7.8–14 wt.% $NaCl_{eq}$ (Type-IIa) to 1.65–6.37 wt.% $NaCl_{eq}$ (Type-IIb) with accuracy ± 0.4 wt.% $NaCl_{eq}$.

Type-I and Type-IIa primary fluid inclusions are hosted in peak minerals (garnet and quartz included in garnet), therefore they were likely entrapped at, or near to, peak P-T conditions. The dominantly aqueous fluid of both Type-I and Type-IIa inclusions was most likely produced through metamorphic devolatilization reactions occurring in the subducting slab. Despite their primary nature, the isochores of Type-I and Type-IIa inclusions do not intersect the peak metamorphic conditions of the blueschist mineral assemblage, suggesting that these inclusions stretched or re-equilibrated during nearly isothermal decompression from 19 kbar to 3 kbar or

less, at $T=290^{\circ}\text{C}$. This conclusion is further supported by their large variability in shapes and sizes which range from irregular inclusions ('C'/arc shaped, hook shape and satellite type). This decompression stage was followed by nearly isobaric cooling, testified by the occurrence of dendritic networks of decrepitated and 'imploded' fluid inclusions.

Key Words: Fluid inclusions, Blueschist, lawsonite, Ladakh, Himalaya

1. Introduction

Fluid inclusions occurring in high pressure – low temperature (HP-LT) metamorphic rocks reveal the nature of fluid as well as the role of fluid in the subduction history of continental or oceanic crust. Fluid inclusions can also be used as a marker point in constraining parts of the P – T paths of different metamorphic rocks (e.g. Hollister et al., 1979; Santosh, 1987; Hames et al., 1989; Sisson et al., 1989; Vry and Brown, 1991; Winslow et al., 1994). Additionally, evidences of fluid–rock interactions occurred during blueschist- and eclogite- facies metamorphism can provide significant insights for our understanding of fluid storage and recycling during subduction or continent-continent collision processes (Brunnsman et al., 2000; Scambelluri and Phillipott, 2001).

The post-entrapment modification of the size and shape of fluid inclusions in response to deformation, cooling or decompression can help to constrain the P - T paths of their host rocks and hence provide some insights on their exhumation processes (e.g. Scambelluri, 1992; Winslow et al., 1994, Vallis and Scambelluri, 1996; Kuster and Stockhert, 1997; El-Shazly and Sisson, 1999; Bakker and Mamtani, 2000). The detailed observation of the fluid inclusion textures and microthermometric results hold the key to fruitful data elucidation (e.g. Bodnar et al., 1989; Sterner and Bodnar, 1989; Vityk et al., 1994; 1995; Barker, 1995; Sterner et al., 1995; Vityk and Bodnar, 1995; Van den Kerkhof and Hein, 2001).

Fluid inclusion studies on subduction-related metamorphic rocks often revealed that the fluid was retained within the subducting slab and that the fluid flow was limited (e.g. El-Shazly and Sisson, 1999; Xiao et al., 2000; Gao and Klemnd, 2001). However, previous fluid inclusion studies focused on HP-LT metamorphic terranes show no general agreement on fluid composition and mechanisms of fluid flow.

Blueschists occur in many orogenic belts including the Pacific, Alpine-Himalayan and Precambrian-Phanerozoic belts (Liou et al., 1990). Most of the studies on the blueschist-facies rocks are focused on petrology, mineralogy and geochronology (e.g. Martin et al., 2011; Vitale Brovarone et al., 2011; Chantel et al., 2012; Abers et al., 2013; Cao et al., 2013; Kim et al., 2013; Spandler and Pirard, 2013), whereas the application of fluid inclusion studies to blueschist-facies rocks is limited so far to few examples. Luckscheiter and Morteani (1980) noticed the presence of CO₂-H₂O fluids in glaucophane-bearing rocks from the Tauern Window, while Barr (1990) reported the presence of only aqueous fluid in blueschist rocks from Syros. Invernizzi et al. (1996) studied the fluid inclusions in quartz veins hosted within blueschist-facies rocks, and inferred the re-equilibration history of these fluid inclusions in terms of uplift processes. The re-equilibration of the vast majority of primary fluid inclusions in high *P*-low *T* rocks during exhumation is the main cause for the scarcity of such studies (Touret, 1992). However, Vityk et al. (1994) and Vityk and Bodnar (1995) experimental works on synthetic fluid inclusions presented textural benchmarks for recreating sections of *P*-*T* paths and for enhancing tectonic interpretations.

Although the Himalaya is the archetype of collisional orogens, high-pressure metamorphic rocks are rare (e.g. Lombardo and Rolfo, 2000; Guillot et al., 2008). The blueschist-facies rocks in Himalaya are mostly lawsonite-bearing and occur along the Indus Suture Zone in Pakistan (Shangla: Shams, 1972; Frank et al., 1977) and NW India (Sapi-Shergol, Ladakh: Honegger et al., 1989; Groppo et al., 2016; Zildat: Viridi et al., 1977). Few lawsonite- and epidote blueschist-

90 facies rocks are also reported from the eastern portion of the orogen in the Indo-Burmese
91 Ranges (Nagaland Ophiolite Complex: Ghose and Singh, 1980; Chatterjee and Ghose, 2010;
92 Ao and Bhowmik, 2014). The preservation of lawsonite in the blueschists indicates very low
93 geothermal gradients during subduction as well as during exhumation processes. The best
94 occurrence of such lithologies in the Himalaya is that of Sapi-Shergol: a preliminary petrologic
95 study of these blueschists by Honegger et al. (1989) constrained peak P-T conditions at 9-11
96 kbar, 350-450°C (conventional thermobarometry). Groppo et al. (2016) estimated significantly
97 higher pressure (19 kbar, 470°C) for the same unit by using *P-T* pseudosection modelling and
98 suggested a very low geothermal gradient (i.e. 8-9°C/km). Sachan and Mukherjee (2001)
99 preliminarily studied the fluids from quartz veins hosted in the blueschist rocks from Sapi-
100 Shergol and provided comments upon their exhumation history. However, these quartz veins
101 are related to a very late stage of the metamorphic evolution, and consequently do not give any
102 direct clue on the blueschist formation and exhumation.

103 As concerning other subduction-related rocks from the Himalaya, a fluid inclusion study by
104 Mukherjee and Sachan (2009) focusing on the ultra-high pressure eclogites from the Tso
105 Morari, showed the prevalence of high-salinity brine, N₂, CH₄, CO₂ –bearing fluids and low-
106 salinity aqueous fluids. This study shows the complex nature of the fluid involved during deep
107 subduction and exhumation of Indian continental crust. Additionally, Ferrando et al. (2007)
108 reported the presence of pure CO₂ and CO₂-H₂O fluids in granulitized eclogites from eastern
109 Himalaya.

110 This paper is the first systematic fluid inclusion study on the blueschist rocks from Sapi-Shergol
111 ophiolitic mélange (Ladakh Himalaya, NW India). The fluids associated to peak and retrograde
112 metamorphic stages are characterised, and the source of these fluids is assessed. Moreover, the
113 fluid evolution is discussed in relation to the P–T paths inferred by Groppo et al. (2016) on the
114 base of thermodynamic modelling. The results from this study have important implications for

the understanding of the nature and role of fluids during subduction-related metamorphism and the consequent uplift, in the framework of the geodynamic evolution of the Himalayan orogeny.

2. Geological Setting

The blueschists studied in this paper occur along the Indus suture zone in Ladakh, NW India (Fig. 1a). From SE to NW, blueschist-facies lithologies are reported at Zildat, Urtsi, Hinju, and Sapi-Shergol (Honegger et al., 1989). Among these occurrences, the largest one is that of Sapi-Shergol in western Ladakh, south of Kargil. Tectonically, the Sapi–Shergol blueschists belong to a narrow belt and are part of an ophiolitic *mélange* (Honegger et al., 1989) (Fig. 1b).

This ophiolitic *mélange* is thrust over the Kargil Molasse to the west as well as to the north, and it is in contact with the Nindam and Lamayuru Formations to the north and to the south, respectively. To the south, the Triassic limestone of the Zaskar Unit is thrust over the *mélange* (Frank et al., 1977, Honegger et al., 1982). The ophiolitic *mélange* is inferred to be a remnant of a paleo-accretionary prism produced by the northward subduction of the Neotethys, originally separating the Ladakh arc to the south from the Asian active margin to the north (Mahéo et al., 2006) (Fig.1a). This paleo-accretionary prism comprises sedimentary bodies including mainly basic lithologies that have been metamorphosed under low-grade to lawsonite blueschist-facies conditions (Frank et al., 1977; Honegger et al., 1989; Reuber et al., 1987; Ahmad et al., 1996; Rolfo et al., 1997; Robertson, 2000; Mahéo et al., 2006). The Sapi–Shergol ophiolitic *mélange* therefore shows a complex internal architecture, including a number of slivers of the paleo-accretionary prism, intercalated with numerous slivers of other units including the Nindam and Lamayuru Formations, as well as low-grade meta-ophiolitic rocks with serpentinitized peridotites intruded by basic dikes (“sheared serpentinites” of Robertson, 2000).

The protoliths of the blueschist lithologies cropping out around the Shergol village are mainly basic metavolcanics and volcanoclastites with subordinate amounts of cherts, metasediments and minor carbonatic lithologies. Mahéo et al. (2006) suggested that the blueschists originate from calc-alkaline igneous rocks formed in an intra-oceanic arc environment. Whole-rock and glaucophane K–Ar geochronology gave an age of ca. 100 Ma for the high-pressure metamorphic peak (Honegger et al., 1989). Petrographically, metabasic rocks are mainly fine-grained glaucophane -bearing schists, with lawsonite and minor clinopyroxene and phengite. Metavolcanoclastic rocks show a clastic structure with irregular fragments of metabasic rocks set in a very fine-grained matrix. The clasts generally contain a blue amphibole + lawsonite ± clinopyroxene assemblage. The matrix is very fine-grained and mainly comprises blue amphibole, chlorite and minor aegirine.

Silicic and impure carbonatic metasediments are locally found as intercalations within the metabasic and metavolcanoclastic rocks. The silicic metasediments comprise glaucophane + lawsonite + phengite ± garnet schists, lawsonite + glaucophane + phengite + garnet quartzitic micaschists and glaucophane + garnet + phengite quartzites. Lawsonite and garnet are either fine-grained or porphyroblastic. Lawsonite and garnet porphyroblasts are from few centimeters to few millimeters in size, and generally overgrow the main foliation. The impure carbonatic metasediments are very fine-grained and mainly consist of lawsonite, calcite, glaucophane, and minor phengite ± prehnite.

3. Petrography

A detailed petrographic study of two representative samples of metasediments (samples 14-4B and 14-6F/G) has been carried out. These metapelites are mainly composed of lawsonite, glaucophane, garnet, phengite and quartz, with minor calcite concentrated in late veins.

Accessory minerals are titanite and pyrite. Both samples are very fresh, one of them being relatively fine-grained (sample 14-4B) compared to the other (sample 14-16F/G).

Sample 14-4B is characterised by alternating layers rich in quartz or lawsonite + glaucophane + phengite, respectively (Fig. 2a, b). Glaucophane occurs in both layers as fine-grained idioblasts; it shows characteristic zoning pattern with light blue core and a dark blue rim. The preferred orientation of glaucophane and phengite defines the main foliation. Garnet is weakly zoned and occurs as small idioblasts (Fig. 2b). Lawsonite occurs as fine-grained idioblasts (Fig. 2c); it contains inclusions of quartz and titanite. In the quartz-rich layers, lawsonite locally shows a skeletal habit, being intergrown with quartz.

The main assemblage of sample 14-6F/G is lawsonite + glaucophane + phengite + garnet + quartz, with glaucophane occurring as a major constituent (Fig. 2d). Titanite occurs as accessory mineral. The main foliation, defined by the preferred orientation of glaucophane and minor phengite, is overgrown by lawsonite and garnet porphyroblasts and is locally crenulated (Fig. 2d, e, f). The growth of lawsonite and garnet porphyroblasts pre-dated the crenulation event. Garnet occurs as medium- to coarse-grained idioblasts (Fig. 2e) locally included within the lawsonite porphyroblasts, and shows strong zoning. Variably sized inclusions of glaucophane, actinolite, phengite, quartz, chlorite and rare omphacite are found in garnet porphyroblasts. Glaucophane occurs as fine-grained nematoblasts in the matrix. Porphyroblastic lawsonite is up to 1 centimetre in size and sub-idioblastic, and overgrows the main foliation. Phengite is fine- to medium-grained and is found in association with glaucophane (Fig. 2d). The main foliation is locally crosscut by quartz \pm albite \pm chlorite veins (Fig. 2f). It is worth noting that in both samples, garnet was predicted to have grown at (or close to) peak P-T conditions, i.e. in the narrow P-T range of 400-470°C, 17-19 kbar (Groppo et al., 2016).

4. Methods

Double polished wafers with a thickness of about 0.4 ± 0.2 mm were prepared from the samples described in chapter 3. A microthermometric study was conducted on a Linkam THMSG 600 stage mounted on Olympus microscope at the Wadia Institute Fluid inclusion Laboratory. The equations of Zhang and Frantz (1987) and Brown and Lamb (1989) were used for the estimation of isochores of aqueous fluid inclusions, whereas the equation of Bower and Helgeson (1985) was used for the calculation of isochores of CO_2 – H_2O inclusions in the “Flinco” computer program of Brown (1989).

5. Fluid inclusion petrography

We have studied fluid inclusions hosted in garnet and in matrix quartz, as well as in quartz included in garnet porphyroblasts belonging to the peak metamorphic mineral assemblage (i.e. garnet + lawsonite + glaucophane + phengite + quartz \pm omphacite; see Groppo et al., 2016). Texturally, two types of fluid inclusions have been found: regular shaped inclusions (Type-I and Type-II) and re-equilibrated inclusions (Type-III). Regular shaped inclusions are either two-phase carbonic-aqueous (Type-I) or two-phase aqueous (Type-II) inclusions. Type-II inclusions are more abundant than Type-I inclusions.

Type-I inclusions are two-phase inclusions ($V_{\text{CO}_2} + L_{\text{H}_2\text{O}}$) at room temperature ($\sim 27^\circ\text{C}$) and contain an aqueous-carbonic fluid (Fig. 3A, B). The size of these inclusions are small (average of $9\ \mu\text{m}$). The CO_2 vapour has a variable volume proportion ranging from 10 to 30% of the total volume of the inclusion. These inclusions are systematically found as isolated occurrences within garnet and quartz, and are dispersed randomly in the host grains (Fig. 3A, B), therefore they have been interpreted as primary in origin; moreover, because garnet is a peak phase, Type-I inclusions have been entrapped at peak P-T conditions.

Type-II inclusions are two-phase aqueous ($V_{\text{H}_2\text{O}} + L_{\text{H}_2\text{O}}$) inclusions and are further classified as Type-IIa and Type-IIb on the basis of their mode of occurrence. The size of these types of

inclusion ranges between 9 and 15 μm . Type-IIa inclusions are isolated and randomly distributed in the matrix quartz as well as in quartz included in garnet grains, and are therefore interpreted as primary inclusions; they were likely entrapped at, or near to, peak P-T conditions because quartz included in garnet is a prograde-to-peak phase. Type-IIb are concentrated along microfractures of the host minerals and are interpreted as secondary inclusions. The trails of the secondary inclusions often cross-cut the grain margins (i.e. transgranular inclusions) (Fig. 3C, D).

Type-III inclusions are re-equilibrated inclusions showing partially dendritic type network as well as necking phenomena (Fig. 4A-D). The dendritic type network may be originated by the dissolution of inclusion walls, as well as by the closing of inclusion voids which lead to form numerous tails and channels filled by fluids (Invernizzi et al., 1998). Some inclusions show necking phenomena, and few also show “C” type microstructures. Some solitary inclusions surrounded by minute satellite inclusions are observed in matrix quartz.

6. Microthermometric results

Microthermometry reveals compositional variations of the fluid inclusions from aqueous-carbonic to aqueous. The results of microthermometric measurements are shown in histograms (Figs. 5, 6 and 7) and summarized in Table 1. The Type-I aqueous-carbonic fluid inclusions hosted in the matrix quartz as well as in quartz included in garnet and in garnet itself, show initial melting temperature (T_{im}) between -56.9°C and -56.6°C , thus suggesting a nearly pure CO_2 composition for the vapour phase. The homogenization temperature of CO_2 in these inclusions lies between -7 to -2°C (Fig. 5B). The clathrate melting temperature was also observed in some carbonic-aqueous inclusions, which occurred between $+7.1$ to 8.6°C . The total homogenization of such inclusions took place in between 227° and 265°C (Fig. 5A).

The Type-II two-phase aqueous inclusions mainly occur in matrix quartz as well as in quartz included in garnet. Type-IIa primary inclusions and Type-IIb secondary inclusions show different initial melting temperature (T_{im}) and final melting temperature (T_{fm}) values. Type IIa primary H_2O -NaCl inclusions show T_{im} in the range $-21.2^{\circ}C$ to $-22.6^{\circ}C$, T_{fm} of $-5^{\circ}C$ to $-10^{\circ}C$ (Fig. 6A) and temperature of homogenization (T_h) between $250^{\circ}C$ and $300^{\circ}C$ (Fig. 7B). The corresponding salinity ranges are estimated at 7.8–13.98 wt% NaCl equivalent, with density of 0.863–0.874 g/cm³. Type-IIb secondary two-phase aqueous inclusions occurring in transgranular trails show a wider range of T_{im} (-21° to $-23^{\circ}C$), and significantly different T_{fm} (-1° to $-4^{\circ}C$; Fig. 6 B) and T_h (145° to $220^{\circ}C$; Fig. 7A) values. The corresponding salinity ranges are estimated at 1.65–6.37 wt% NaCl equivalent, and density is in the range of 0.889–0.938 g/cm³.

Composition and density of the fluid phase observed in the different generations of inclusions are used to calculate the isochores in the P – T space, and the implications are discussed in a later section. The minimum T_h and the maximum T_h obtained from the peak value in Figs. 5,6,7 for each inclusion type were considered for construction of isochores, following the criteria given by Touret (2001),.

7. Discussion

The study of fluid inclusions provides important constraints on their trapping conditions (textural evidence in relation to P – T estimates), composition and behaviour of metamorphic fluids. This is the first systematic fluid inclusion study on the blueschists from the Sapi-Shergol ophiolitic mélange that correlates P - T data from mineral geothermobarometry and fluid inclusions. Our results reveal the pervasive presence of aqueous-carbonic and aqueous fluids preserved in quartz and garnet.

7.1. *Interpretation of fluid inclusions textures*

In the studied samples, the isolated nature of Type-I aqueous-carbonic inclusions and of Type-IIa two-phase aqueous inclusions hosted in quartz and garnet reveals that they may have formed during the crystallization of their host minerals, and may thus be considered to be trapped early during the mineral growth (Roedder, 1984). Moreover, because garnet is a peak phase, the primary Type-I and Type-IIa inclusions have been entrapped at, or near to, peak P-T conditions. Type-IIb two-phase aqueous inclusions occur in transgranular trails and are therefore clearly secondary in nature.

Concerning Type-III inclusions, the most commonly observed features are: (i) necking, (ii) inclusions with 'C' or Arc shaped microstructure, (iii) satellite inclusions, (iv) hook shaped or annular inclusions, (v) dendritic network of inclusions (Fig.4 A, B, C & D). The necking textures are interpreted as related to intense dissolution of the inclusion walls to produce highly irregular inclusion morphology. These microtextures were likely formed along a decompression path: fractures initially developed along the inclusion planes in which inclusions primarily necked down, and later on they were stretched (Fig 4C). The inclusions displaying a hook-like morphology or annular textures (Fig.4C) are similar to inclusions formed under isothermal decompression (ITD), as shown in the experimental work of Sterner and Bodnar (1989), Vityk and Bodnar (1995), and Bodnar (2003). Boullier et al. (1991) proposed that annular textures are symptomatic of an anisotropic stress environment. Satellite inclusions around a bigger solitary inclusion are analogous to 'explosion' textures described for natural and synthetic fluid inclusions in quartz that have experienced overpressures caused by 'near isothermal decompression' (e.g., Bodnar et al., 1989; Vityk et al., 1994; Vityk and Bodnar, 1995). Opposite to these microtextures which are related to decompression, the development of dendritic networks of imploded inclusions in quartz is indicative of near isobaric cooling (IBC) in the last stages of metamorphic evolution. This type of texture is similar to that described by Vityk

et al. (1994) and Vityk and Bodnar (1995) for their experimental work during isobaric cooling (IBC).

7.2. Nature and Source of Fluids

Two types of fluid (aqueous-carbonic and aqueous) have been found in the blueschist mineral assemblage. Type-I aqueous-carbonic fluids occur as primary inclusions in peak metamorphic garnet as well as in quartz. Type-IIa aqueous fluid with high saline nature is preserved as primary inclusions in matrix quartz, as well as in quartz included in garnet, whereas Type-IIb aqueous fluid with low saline nature is observed as secondary inclusions in quartz.

Type-I aqueous-carbonic inclusions have constant vapour: liquid ratios (i.e. 30:70). The temperature of clathrate melting and the homogenization temperature of the CO₂ phase in these inclusions indicate that they are predominantly aqueous with a small amount of CO₂, consistently with the stability of lawsonite at peak metamorphic conditions. According to Groppo et al. (2016), in fact, the contemporaneous growth of lawsonite and garnet would have been enhanced by a protracted H₂O influx at the relatively high pressure of ca. 17–18 kbar. The predominance of aqueous fluids in high P metamorphic assemblages is also shown in previous studies which call upon substantial fluid release at high P–T conditions (e.g. Clarke et al., 2006; Tsujimori and Ernst, 2014; Ulmer and Trommsdorff, 1995; Scambelluri et al., 2004; Poli and Schmidt, 1995; Poli et al., 2009) through metamorphic devolatilization reactions occurring in the subducting slab (Bebout, 1991, 1995; Jarrard, 2003).

7.3. Reconstruction of the P-T-fluid history

P–T estimates based on conventional thermobarometry proposed peak conditions of 350–420 °C, 9–11 kbar for the Sapi-Shergol blueschists (Honegger et al., 1989). Petrologic modeling performed by our research team (Groppo et al., 2016) inferred peak P–T conditions significantly

312 higher than those previously estimated, i.e. ca. 470 °C, 19 kbar. According to Groppo et al.
313 (2016), the estimated peak metamorphic conditions suggest that the blueschists experienced a
314 cold subduction history along a very low to low thermal gradient (“early” prograde: ca. 5–6
315 °C/km; “late” prograde: ca. 7–8 °C/km). The preservation of lawsonite in the studied lithologies
316 further indicate that the exhumation process must have been coupled with substantial cooling
317 (i.e. without crossing the lawsonite-out boundary; Zack et al., 2004).

318 As concerning the fluid evolution, isochores are plotted in comparison with the P – T path
319 inferred on the basis of thermodynamic modelling and thermobarometry (Fig. 8). Isochores of
320 both Type-I aqueous–carbonic inclusions and Type-II aqueous inclusions plot in the lower part
321 of the P – T space. Although these inclusions are texturally primary and are hosted within peak
322 minerals (garnet and quartz included in garnet), they do not plot along the prograde P – T path
323 or at peak metamorphic conditions, thus suggesting that these inclusions must have experienced
324 considerable leakage and re-equilibration, resulting in only low-density fluid eventually
325 preserved in the inclusions. Therefore, it is assumed that Type-I CO_2 – H_2O and Type-IIa aqueous
326 inclusions most likely formed at or near the peak P – T conditions at ~ 19 kbar, ~ 450°C, but
327 they were later re-equilibrated during exhumation. The isochores of secondary aqueous
328 inclusions (Type IIa) plots above the isochores of primary inclusions because the secondary
329 aqueous inclusions originate at lower temperature and their densities are thus higher (Fig.8).

330 Evidences of such a pervasive re-equilibration are very clearly represented by the textural
331 features of Type-III fluid inclusions described in the previous chapters (Fig.4). The observed
332 textural features are indicative either of re-equilibration occurred during isothermal
333 decompression, as well as during isobaric cooling at the final stages of exhumation. Similar
334 high degrees of re-equilibration of fluid inclusions during retrogression is well documented by
335 Sterner and Bodnar (1989) and Kuster and Stockhert (1997) for high- P and low- T rocks. We
336 therefore suggest that these re-equilibrated inclusions might have been trapped during the early

stages of subduction, while their re-equilibration took place during the subsequent fast exhumation. Such high internal underpressure at low temperature would develop only when the subduction / burial path is very steep and consequently follows very low geothermal gradients; the preservation of lawsonite in the studied blueschist facies lithologies strongly support the scenario in which very low geothermal gradients were prevailing during initial subduction as well as during exhumation (Fig. 8). The presence of dendritic network type inclusions suggests isobaric cooling (as evidenced by the experimental studies of Bodnar et al., 1989; Vityk et al., 1994; Vityk and Bodnar, 1995). The hook like inclusions were likely trapped at about 3 kbar (Vityk and Bodnar, 1995), whereas the implosion texture formed at higher pressure (Boulier, 1999). In our case, the last stage of the P-T evolution is represented by the isobaric cooling after the isothermal decompression, therefore we suggest that the dendritic morphology might have been formed at this last stage (Fig. 8). This interpretation is clearly compatible with the broad geological setting of the area.

8. Conclusions

The first detailed fluid inclusions study of Himalayan blueschist-facies lithologies from the Sapi-Shergol ophiolitic mélange in the Indus suture zone, revealed predominantly CO₂-H₂O and H₂O-NaCl inclusions. The primary CO₂-H₂O and H₂O-NaCl inclusions were trapped by host minerals at peak P-T conditions. The fluid was most likely produced through metamorphic devolatilization reactions occurring in the subducting slab. Additional multiple generations of re-equilibrated inclusions show characteristic morphologies developed in response to fast rates of uplift. A nearly isothermal decompression path followed peak metamorphic P-T condition and is characterized by stretching, necking and formation of “C” or hook-like shaped inclusions. A veining stage is associated to late isobaric cooling and is characterized by the local development of a dendritic network of fluid inclusions.

362

363 **Acknowledgments**

364 HKS, AK, PCS and ST are thankful to the Director of the Wadia Institute of Himalayan
365 Geology, Dehradun, for providing lab facilities and encouragement to carry out this work. An
366 nonymous reviewer and the journal editor provided useful suggestions, which led to significant
367 improvement of the manuscript. This study is part of a Cooperation Agreement between the
368 Wadia Institute of Himalayan Geology (Dehradun, India) and the University of Torino, Dept.
369 of Earth Sciences (Torino, Italy). Fieldwork of FR and CG was supported by University of
370 Torino—Call 1—Junior PI Grant (TO_Call1_2012_0068).

References

- Abers, G. A., Nakajima, J., van Keken, P. E., Kita, S., Hacker, B. R., 2013. Thermal–petrological controls on the location of earthquakes within subducting plates. *Earth and Planetary Science Letters* 369, 178-187.
- Ahmad, T., Islam, R., Khanna, P. P., Thakur, V. C., 1996. Geochemistry, petrogenesis and tectonic significance of the basic volcanic units of the Zildat ophiolitic mélange, Indus suture zone, eastern Ladakh (India). *Geodinamica Acta* 9, 222-233.
- Ao, A., Bhowmik, S. K., 2014. Cold subduction of the Neotethys: the metamorphic record from finely banded lawsonite and epidote blueschists and associated metabasalts of the Nagaland Ophiolite Complex, India. *Journal of Metamorphic Geology* 32, 829-860.
- Bakker, R. J., Mamtani, M. A., 2000. Fluid inclusions as metamorphic process indicators in the Southern Aravalli Mountain Belt (India). *Contributions to Mineralogy and Petrology* 139, 163-179.
- Barker, A. J., 1995. Post-entrapment modification of fluid inclusions due to overpressure: evidence from natural samples. *Journal of Metamorphic Geology* 13, 737-750.
- Barr, H., 1990. Preliminary fluid inclusion studies in a high-grade blueschist terrain, Syros, Greece. *Mineralogical Magazine* 54, 159-168.
- Bebout, G. E., 1991. Field-based evidence for devolatilization in subduction zones: Implications for arc magmatism. *Science* 251, 413-416.
- Bebout, G. E., 1995. The impact of subduction-zone metamorphism on mantle-ocean chemical cycling. *Chemical Geology* 126, 191-218.
- Bodnar, R. J., 2003. Re-equilibration of fluid inclusions. *Fluid inclusions: Analysis and interpretation* 32, 213-230.

394 Bodnar, R. J., Binns, P. R., Hall, D. L., 1989. Synthetic fluid inclusions-VI. Quantitative
 395 evaluation of the decrepitation behaviour of fluid inclusions in quartz at one atmosphere
 396 confining pressure. *Journal of Metamorphic Geology* 7, 229-242.

397 Boullier, A. M., France-Lanord, C., Dubessy, J., Adamy, J., Champenois, M., 1991. Linked
 398 fluid and tectonic evolution in the High Himalaya mountains (Nepal). *Contributions to*
 399 *Mineralogy and Petrology* 107, 358-372.

400 Bowers, T. S., Helgeson, H. C., 1983. Calculation of the thermodynamic and geochemical
 401 consequences of nonideal mixing in the system $\text{H}_2\text{O}-\text{CO}_2-\text{NaCl}$ on phase relations in geologic
 402 systems: Equation of state for $\text{H}_2\text{O}-\text{CO}_2-\text{NaCl}$ fluids at high pressures and temperatures.
 403 *Geochimica et Cosmochimica Acta* 47, 1247-1275.

404 Brovarone, A. V., Groppo, C., Hetényi, G., Compagnoni, R., Malavieille, J., 2011. Coexistence
 405 of lawsonite-bearing eclogite and blueschist: phase equilibria modelling of Alpine Corsica
 406 metabasalts and petrological evolution of subducting slabs. *Journal of Metamorphic Geology*
 407 29, 583-600.

408 Brown, P. E., 1989. FLINCOR; a microcomputer program for the reduction and investigation
 409 of fluid-inclusion data. *American Mineralogist* 74, 1390-1393.

410 Brown, P. E., Lamb, W. M., 1989. P-V-T properties of fluids in the system $\text{H}_2\text{O}\pm\text{CO}_2\pm\text{NaCl}$:
 411 New graphical presentations and implications for fluid inclusion studies. *Geochimica et*
 412 *Cosmochimica Acta* 53, 1209-1221.

413 Cao, Y., Jung, H., Song, S., 2013. Petro-fabrics and seismic properties of blueschist and eclogite
 414 in the North Qilian suture zone, NW China: Implications for the low-velocity upper layer in
 415 subducting slab, trench-parallel seismic anisotropy, and eclogite detectability in the subduction
 416 zone. *Journal of Geophysical Research: Solid Earth* 118, 3037-3058.

417 Chantel, J., Mookherjee, M., Frost, D. J., 2012. The elasticity of lawsonite at high pressure and
 418 the origin of low velocity layers in subduction zones. *Earth and Planetary Science Letters* 349,
 419 116-125.

420 Chatterjee, N., Ghose, N. C., 2010. Metamorphic evolution of the Naga Hills eclogite and
 421 blueschist, Northeast India: implications for early subduction of the Indian plate under the
 422 Burma microplate. *Journal of Metamorphic Geology* 28, 209-225.

423 Clarke, G. L., Powell, R., Fitzherbert, J. A., 2006. The lawsonite paradox: a comparison of field
 424 evidence and mineral equilibria modelling. *Journal of Metamorphic Geology* 24, 715-725.

425 El-Shazly, A. K., Sisson, V. B., 1999. Retrograde evolution of eclogite facies rocks from NE
 426 Oman: evidence from fluid inclusions and petrological data. *Chemical Geology* 154, 193-223.

427 Ferrando, S., Rolfo, F., Lombardo, B., 2007. Fluid evolution from metamorphic peak to
 428 exhumation in Himalayan granulitised eclogites, Ama Drime range, southern Tibet. *Eur. J.*
 429 *Mineral.* 19, 439–461.

430 Frank, W., Gansser, A., Trommsdorff, V., 1977. Geological observations in the Ladakh area
 431 (Himalayas): a preliminary report. *Schweiz. mineral. petrogr. Mitt* 57, 89-113.

432 Gao, J., Klemd, R., 2001. Primary fluids entrapped at blueschist to eclogite transition: evidence
 433 from the Tianshan meta-subduction complex in northwestern China. *Contributions to*
 434 *Mineralogy and Petrology* 142, 1-14.

435 Ghose, N. C., Singh, M. R., 1980. Occurrence of blueschist facies in the ophiolite belt of Naga
 436 Hills, east of Kiphire, NE India. *Geologische Rundschau* 69, 41-48.

437 Giaramita, M. J., Sorensen, S. S., 1994. Primary fluids in low-temperature eclogites: evidence
 438 from two subduction complexes (Dominican Republic, and California, USA). *Contributions to*
 439 *Mineralogy and Petrology* 117, 279-292.

440 Groppo, C., Rolfo, F., Sachan, H. K., Rai, S. K., 2016. Petrology of blueschist from the Western
 441 Himalaya (Ladakh, NW India): Exploring the complex behavior of a lawsonite-bearing system
 442 in a paleo-accretionary setting. *Lithos* 252, 41-56.

443 Guillot, S., Mahéo, G., de Sigoyer, J., Hattori, K.H. Pecher, A., 2008. Tethyan and Indian
 444 subduction viewed from the Himalayan high- to ultrahigh-pressure metamorphic rocks.
 445 *Tectonophysics* 451, 225–241.

446 Hames, W. E., Tracy, R. J., Bodnar, R. J., 1989. Postmetamorphic unroofing history deduced
 447 from petrology, fluid inclusions, thermochronometry, and thermal modeling: An example from
 448 southwestern New England. *Geology* 17, 727-730.

449 Hollister, L. S., Burruss, R. C., Henry, D. L., Hendel, E. M., 1979. Physical conditions during
 450 uplift of metamorphic terranes, as recorded by fluid inclusions. *Bulletin de Mineralogie* 102,
 451 555-561.

452 Honegger, K., Le Fort, P., Mascle, G., Zimmermann, J. L., 1989. The blueschists along the
 453 Indus suture zone in Ladakh, NW Himalaya. *Journal of Metamorphic Geology* 7, 57-72.

454 Invernizzi, C., Vityk, M., Cello, G., Bodnar, R., 1998. Fluid inclusions in high pressure/low
 455 temperature rocks from the Calabrian Arc (Southern Italy): the burial and exhumation history
 456 of the subduction-related Diamante-Terranova unit. *Journal of Metamorphic Geology* 16, 247-
 457 258.

458 Jarrard, R. D., 2003. Subduction fluxes of water, carbon dioxide, chlorine, and potassium.
 459 *Geochemistry, Geophysics, Geosystems*, 4(5).

460 Kim, D., Katayama, I., Michibayashi, K., Tsujimori, T., 2013. Deformation fabrics of natural
 461 blueschists and implications for seismic anisotropy in subducting oceanic crust. *Physics of the*
 462 *Earth and Planetary Interiors* 222, 8-21.

463 Klemm, R., 1989. PT evolution and fluid inclusion characteristics of retrograded eclogites,
 464 Münchberg Gneiss Complex, Germany. *Contributions to Mineralogy and Petrology* 102, 221-
 465 229.

466 Klemm, R., Van den Kerkhof, A. M., Horn, E. E., 1992. High-density CO₂ – N₂ inclusions in
 467 eclogite-facies metasediments of the Münchberg gneiss complex, SE Germany. *Contributions*
 468 *to Mineralogy and Petrology* 111, 409-419.

469 Küster, M., Stöckhert, B., 1997. Density changes of fluid inclusions in high-pressure low-
 470 temperature metamorphic rocks from Crete: a thermobarometric approach based on the creep
 471 strength of the host minerals. *Lithos* 41, 151-167.

472 Lombardo, B. Rolfo, F., 2000. Two contrasting eclogite types in the Himalayas: implications
 473 for the Himalayan orogeny. *Journal of Geodynamics* 30, 37–60.

474 Luckscheiter, B., Morteani, G., 1980. Microthermometrical and chemical studies of fluid
 475 inclusions in minerals from Alpine veins from the penninic rocks of the central and western
 476 Tauern Window (Austria/Italy). *Lithos* 13, 61-77.

477 Mahéo, G., Fayoux, C., Guillot, S., Garzanti, E., Capiez, P., Mascle, G., 2006. Geochemistry
 478 of ophiolitic rocks and blueschists from the Sapi-Shergol mélange (Ladakh, NW Himalaya,
 479 India): implication for the timing of the closure of the Neo-Tethys ocean. *Journal of Asian Earth*
 480 *Sciences* 26, 695-707.

481 Martin, L. A., Wood, B. J., Turner, S., Rushmer, T., 2011. Experimental measurements of trace
 482 element partitioning between lawsonite, zoisite and fluid and their implication for the
 483 composition of arc magmas. *Journal of Petrology*, egr018.

484 Mukherjee, B. K., Sachan, H. K., 2009. Behavior of fluids in coesite bearing rocks of Tso-
 485 Morari region, NW Himalaya: Implication for exhumation process. *Geological Magazine* 146,
 486 876-889.

487 Poli, S., Schmidt, M. W., 1995. H₂O transport and release in subduction zones: experimental
 488 constraints on basaltic and andesitic systems. *Journal of Geophysical Research: Solid Earth*
 489 100(B11), 22299-22314.

490 Poli, S., Franzolin, E., Fumagalli, P., Crottini, A., 2009. The transport of carbon and hydrogen
 491 in subducted oceanic crust: an experimental study to 5 GPa. *Earth and Planetary Science Letters*
 492 278, 350-360.

493 Reuber, I., Colchen, M., Mevel, C., 1987. The geodynamic evolution of the South-Tethyan,
 494 margin in Zaskar, NW-Himalaya, as revealed by the Spongtag ophiolitic mélanges.
 495 *Geodinamica Acta* 1, 283-296.

496 Robertson, A. H. F., 2000. Formation of mélanges in the Indus suture zone, Ladakh Himalaya
 497 by successive subduction-related, collisional and post-collisional processes during late
 498 Mesozoic-late Tertiary time. *Geological Society, London, Special Publications* 170, 333-374.

499 Roedder, E., 1984. *Fluid Inclusions (Reviews in Mineralogy, Vol. 12)* Mineralogical Society
 500 of America. Washington, DC.

501 Rolfo, F., Lombardo, B., Compagnoni, R., Le Fort, P., Lemennicier, Y., Pêcher, A., 1997.
 502 *Geology and Metamorphism of the Ladakh Terrane and Shyok Suture Zone in the Chogo*
 503 *Lungma - Turmik area (northern Pakistan)*. *Geodinamica Acta* 10, 251-270.

504 Sachan, H. K., Mukherjee, B. K., 2001. Evidences of fluid re-equilibration in blueschist rocks
 505 from Shergol Ophiolitic Mélange, Indus Suture Zone, Ladakh. *Himalayan Geology* 22, 127-
 506 133.

507 Santosh, M., 1987. Cordierite gneisses of southern Kerala, India: petrology, fluid inclusions
 508 and implications for crustal uplift history. *Contributions to Mineralogy and Petrology* 96, 343-
 509 356.

510 Scambelluri, M., 1992. Retrograde fluid inclusions in eclogitic metagabbros from the Ligurian
 511 Western Alps. *European journal of mineralogy* 4, 1097-1112.

512 Scambelluri, M., Philippot, P., 2001. Deep fluids in subduction zones. *Lithos* 55, 213-227.

513 Scambelluri, M., Müntener, O., Ottolini, L., Pettke, T. T., Vannucci, R., 2004. The fate of B,
 514 Cl and Li in the subducted oceanic mantle and in the antigorite breakdown fluids. *Earth and*
 515 *Planetary Science Letters* 222, 217-234.

516 Selverstone, J., Spear, F.S., 1985. Metamorphic P–T Paths from pelitic schists and greenstones
 517 from the south-west Tauern Window, Eastern Alps. *Journal of metamorphic Geology* 3, 439-
 518 465.

519 Shams, F. A., 1972. Glaucophane-bearing rocks from near Topsis, Swat. First record from
 520 Pakistan. *Pakistan Journal of Scientific Research* 24, 343-345.

521 Sisson, V. B., Hollister, L. S., Onstott, T. C., 1989. Petrologic and age constraints on the origin
 522 of a low-pressure/high-temperature metamorphic complex, southern Alaska. *Journal of*
 523 *Geophysical Research: Solid Earth* 94(B4), 4392-4410.

524 Spandler, C., Pirard, C., 2013. Element recycling from subducting slabs to arc crust: A review.
 525 *Lithos* 170, 208-223.

526 Sterner, S. M., Bodnar, R. J., 1989. Synthetic fluid inclusions-VII. Re-equilibration of fluid
 527 inclusions in quartz during laboratory-simulated metamorphic burial and uplift. *Journal of*
 528 *Metamorphic Geology* 7, 243-260.

529 Sterner, S. M., Hall, D. L., Keppler, H., 1995. Compositional re-equilibration of fluid inclusions
 530 in quartz. *Contributions to Mineralogy and Petrology* 119, 1-15.

531 Thakur, V., Misra, D., 1984. Tectonic framework of the Indus and Shyok suture zones in eastern
 532 Ladakh, northwest Himalaya. *Tectonophysics* 101, 207-220.

533 Touret, J. L., 2001. Fluids in metamorphic rocks. *Lithos* 55, 1-25.

534 Touret, J., Van Hinte, J. E., 1992. Le rôle des fluides dans les zones de subduction: un séminaire
 535 du Collège de France aux Pays-Bas. *Proceedings of the Koninklijke Nederlandse Akademie*
 536 *van Wetenschappen* 95, 293-296.

537 Tsujimori, T., Ernst, W. G., 2014. Lawsonite blueschists and lawsonite eclogites as proxies for
 538 palaeo-subduction zone processes: a review. *Journal of Metamorphic Geology* 32, 437-454.
 539 Ulmer, P., Trommsdorff, V., 1995. Serpentine stability to mantle depths and subduction-related
 540 magmatism. *Science* 268(5212), 858.
 541 Vallis, F., Scambelluri, M., 1996. Redistribution of high-pressure fluids during retrograde
 542 metamorphism of eclogite-facies rocks (Voltri Massif, Italian Western Alps). *Lithos* 39, 81-92.
 543 Van den Kerkhof, A. M., Hein, U. F., 2001. Fluid inclusion petrography. *Lithos* 55, 27-47.
 544 Viridi, N. S., Thakur, V. C., Kumar, S., 1977. Blueschist facies metamorphism from the Indus
 545 suture zone of Ladakh and its significance. *Himalayan Geology* 7, 479-482.
 546 Vityk, M. O., Bodnar, R. J., 1995. Textural evolution of synthetic fluid inclusions in quartz
 547 during reequilibration, with applications to tectonic reconstruction. *Contributions to*
 548 *Mineralogy and Petrology* 121, 309-323.
 549 Vityk, M. O., Bodnar, R. J., Schmidt, C. S., 1994. Fluid inclusions as tectonothermobarometers:
 550 Relation between pressure-temperature history and reequilibration morphology during crustal
 551 thickening. *Geology* 22, 731-734.
 552 Vry, J. K., Brown, P. E., 1991. Texturally-early fluid inclusions in garnets: evidence of the
 553 prograde metamorphic path? *Contributions to Mineralogy and Petrology* 108, 271-282.
 554 Winslow, D. M., Bodnar, R. J., Tracy, R. J., 1994. Fluid inclusion evidence for an anticlockwise
 555 metamorphic P-T path in central Massachusetts. *Journal of Metamorphic Geology* 12, 361-371.
 556 Xiao, Y., Hoefs, J., van den Kerkhof, A. M., Fiebig, J., Zheng, Y., 2000. Fluid history of UHP
 557 metamorphism in Dabie Shan, China: a fluid inclusion and oxygen isotope study on the coesite-
 558 bearing eclogite from Bixiling. *Contributions to Mineralogy and Petrology* 139, 1-16.
 559 Zack, T., Rivers, T., Brumm, R., Kronz, A., 2004. Cold subduction of oceanic crust:
 560 implications from a lawsonite eclogite from the Dominican Republic. *European Journal of*
 561 *Mineralogy* 16, 909-916.

562 Zhang, Y. G., Frantz, J. D., 1987. Determination of the homogenization temperatures and
563 densities of supercritical fluids in the system NaCl-KCl-CaCl₂-H₂O using synthetic fluid
564 inclusions. Chemical Geology 64, 335-350.

Figure Captions

Figure 1. (A) Regional Geological Map of Ladakh Himalaya (adopted from Thakur and Misra, 1984, and Mahéo et al., 2006); (B) Geological map of Shergol ophiolitic mélange (after Honegger et al., 1989).

Figure 2. Representative microstructures of the studied blueschists. **Sample 14-4B:** (a) Glaucophane + phengite + lawsonite layers alternated to discontinuous quartz-rich layers. Plane Polarized Light (PPL); (b) Glaucophane + phengite + lawsonite layer containing variably sized garnet Crosse Polarized Light (XPL); (c) Fine-grained idioblasts of lawsonite occur in association with glaucophane (PPL); **Sample 14-6F/G:** (d, e) Glaucophane with minor phengite defines the main foliation. The foliation is overgrown by lawsonite and garnet porphyroblasts (PPL); (f) Lawsonite porphyroblast is crosscut by thin quartz veins (XPL).

Figure 3. Representative photomicrographs of Type-I and Type-II fluid inclusions (PPL). (a) Type-I primary two-phase carbonic-aqueous inclusions in garnet (sample14-6F/G). (b) Type-I primary two-phase aqueous-carbonic inclusions in matrix quartz (sample 14-4B). (c) Type-IIa primary two-phase aqueous inclusions in quartz included in garnet (sample14-6F/G). (d) Type-IIb secondary two-phase aqueous inclusions and Type-III re-equilibrated inclusions in quartz (sample 14-4B).

Figure 4. Representative photomicrographs of Type-III fluid inclusions (PPL). (a) Re-equilibrated inclusions in quartz showing implosion textures (sample14-6F/G). (b) Re-equilibrated inclusions in quartz exhibiting necking and dendritic type networks of fluid inclusions (sample14-6F/G). (c) Re-equilibrated inclusion in quartz showing different morphologies: (i) hook-shape microstructure; (ii) “C” or “arc” shape, and (iii) necking and

stretched phenomena (sample 14-4B). **(d)** Dendritic type network of secondary fluid inclusions in quartz (sample 14-4B).

Figure 5. Histograms showing **(a)** homogenization temperature (T_h), and **(b)** final melting temperature of CO_2 for Type-I CO_2 - H_2O primary inclusions hosted in quartz and garnet.

Figure 6. Histograms showing final melting temperature of **(a)** Type-IIa primary H_2O - NaCl inclusions in quartz, and **(b)** Type-IIb secondary H_2O - NaCl inclusions in quartz.

Figure 7. Histograms showing homogenization temperature (T_h) for **(a)** Type-IIa primary H_2O - NaCl inclusions in quartz, and **(b)** Type-IIb secondary H_2O - NaCl inclusions in quartz.

Figure 8. Comparison between fluid inclusion isochores and the P - T path (thick arrow in pink) recorded by blueschist from the Sapi-Shergol ophiolitic mélange (after Groppo et al., 2016). The lawsonite boundary is drawn after Zack et al. (2004). The yellow box shows peak metamorphic conditions. The retrograde path is mainly characterized by nearly isothermal decompression (as evident from hook shaped, annular inclusions and explosion type textures). The last portion of the P - T path is characterized by isobaric cooling (as constrained by the development of dendritic type networks of inclusions).

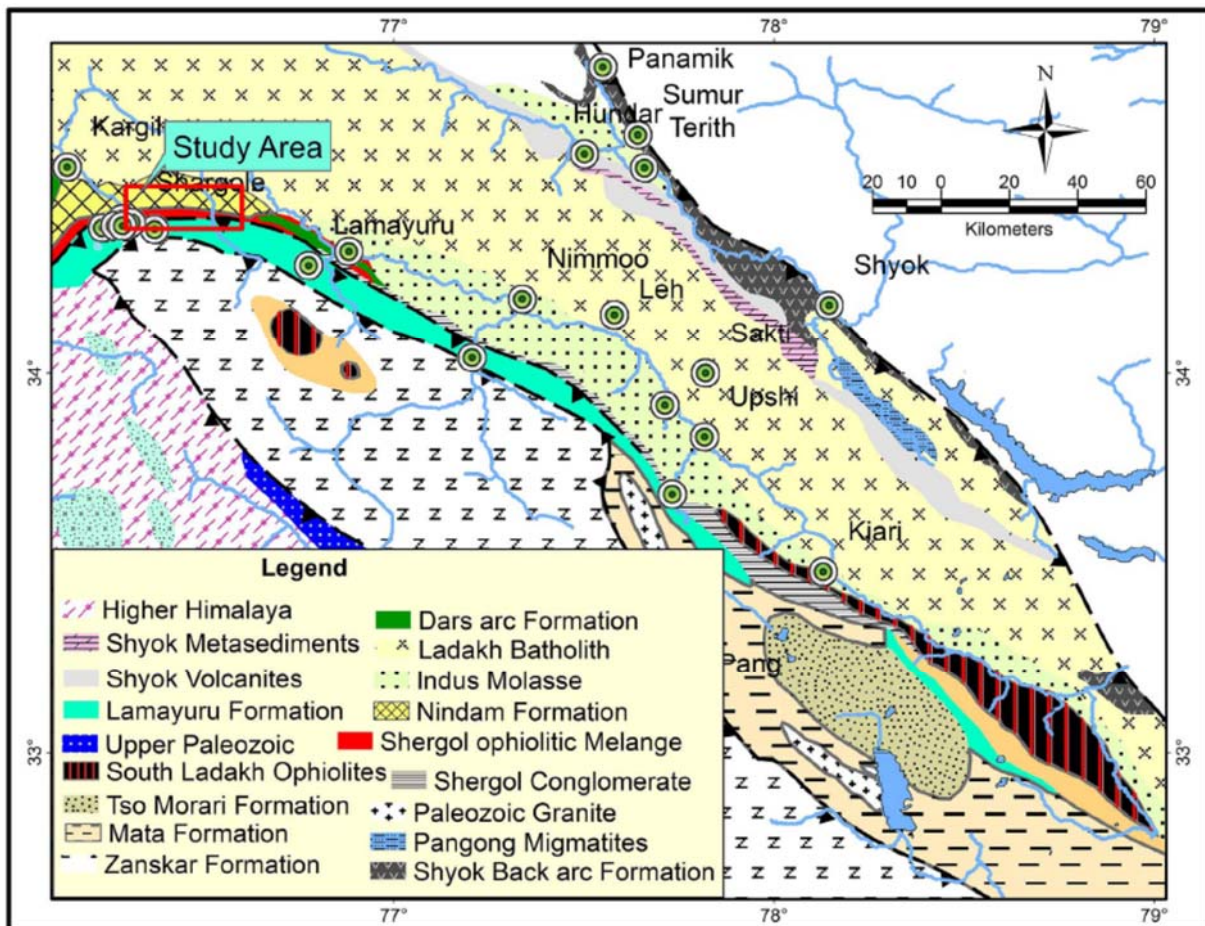


Fig. 1a

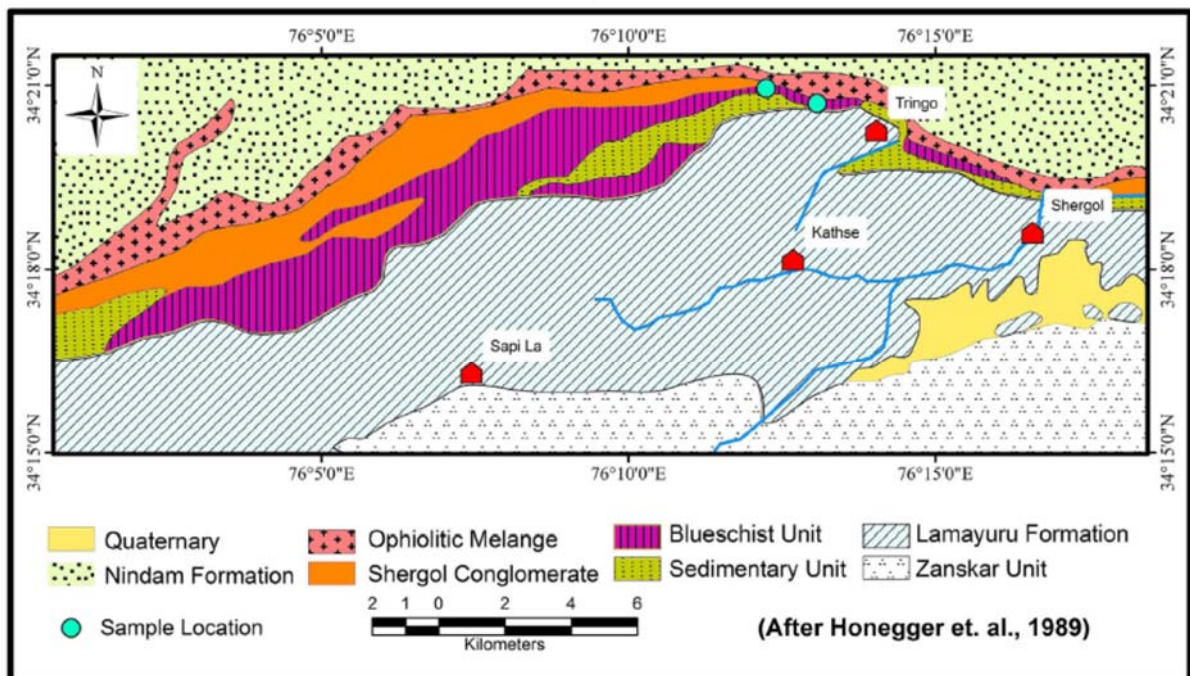


Fig. 1

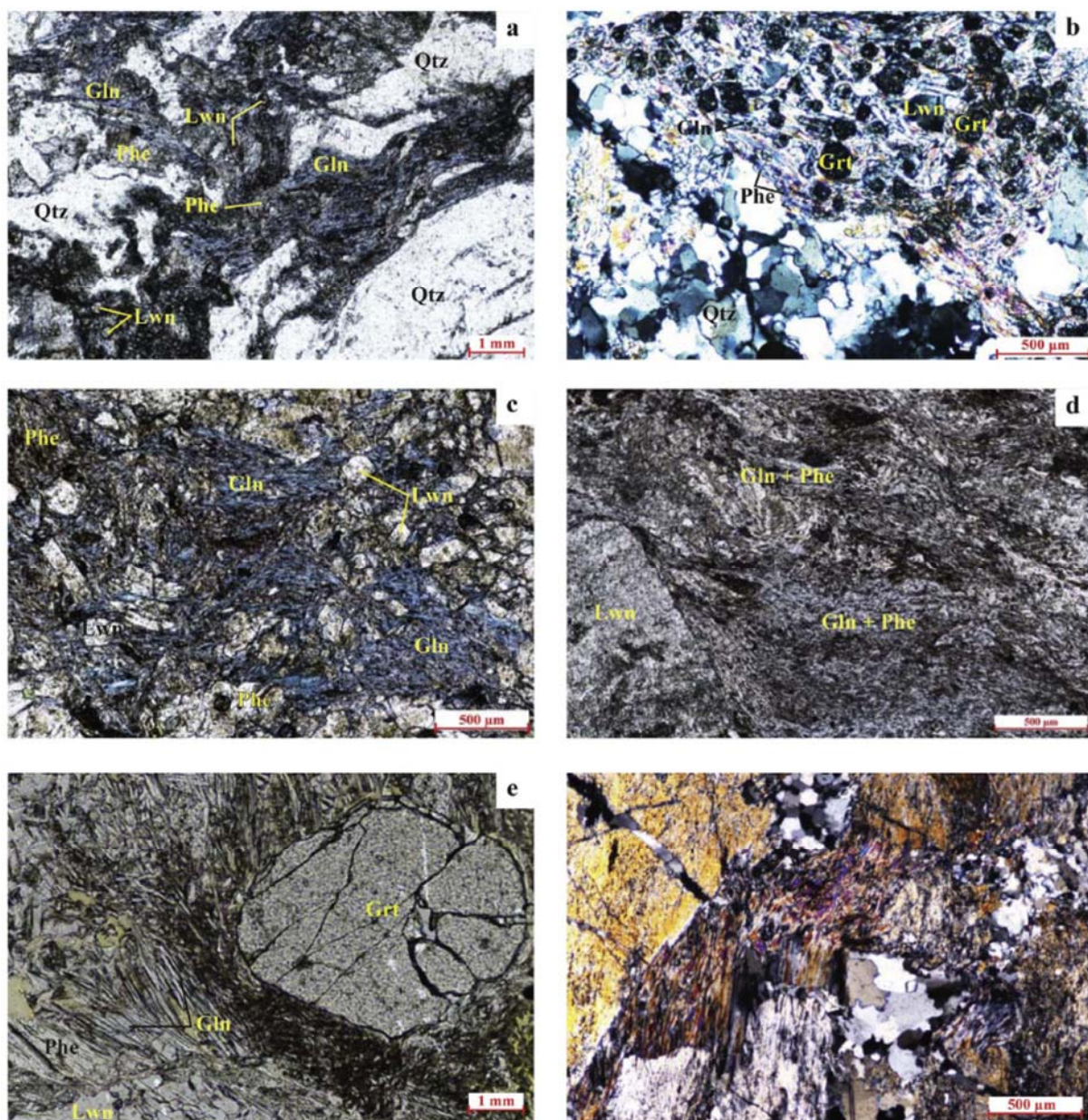


Fig. 2

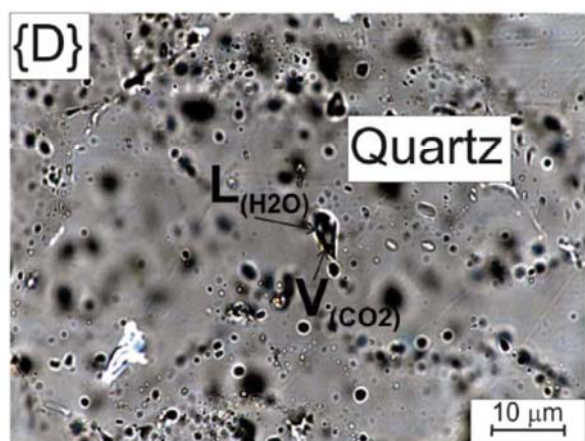
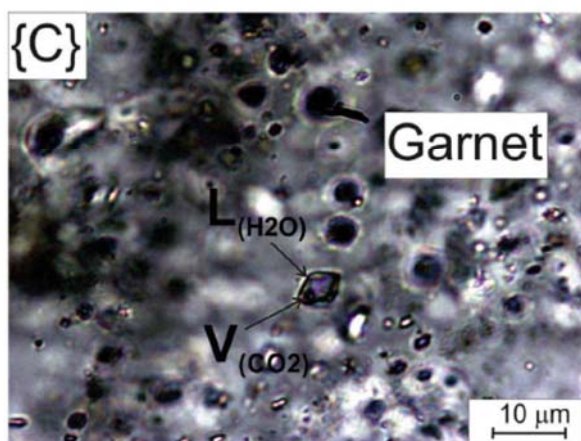
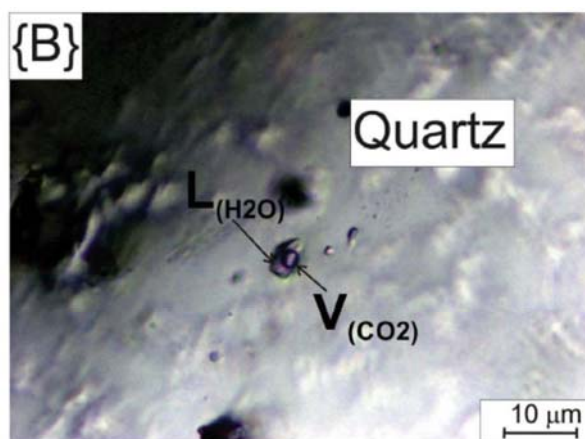
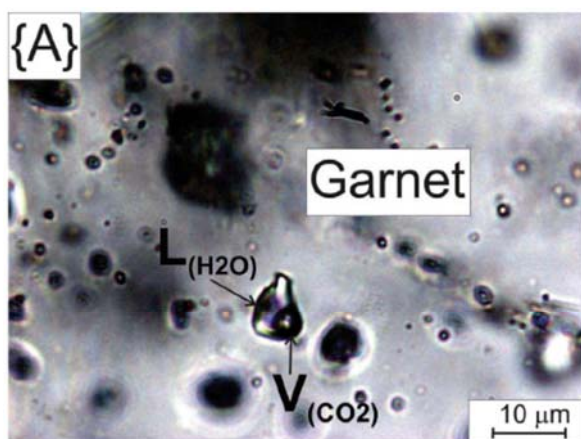


Fig. 3

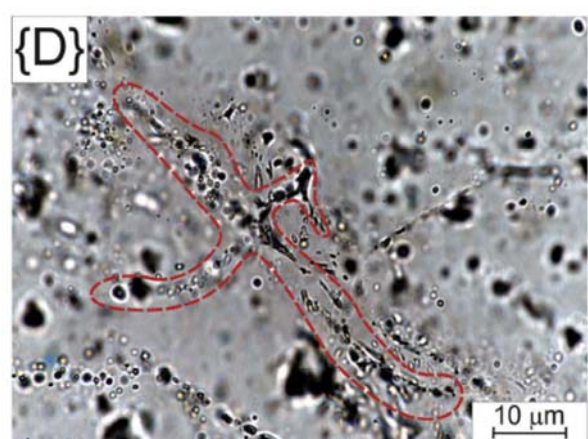
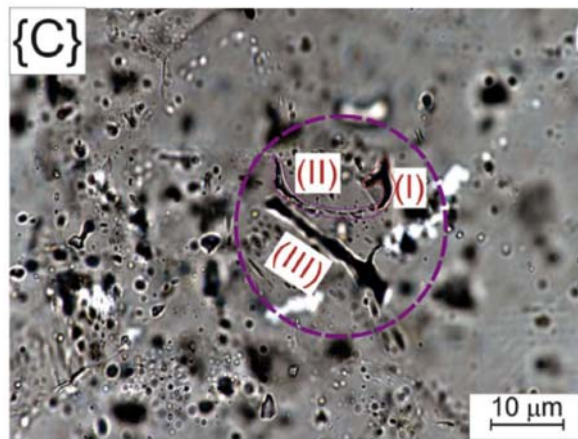
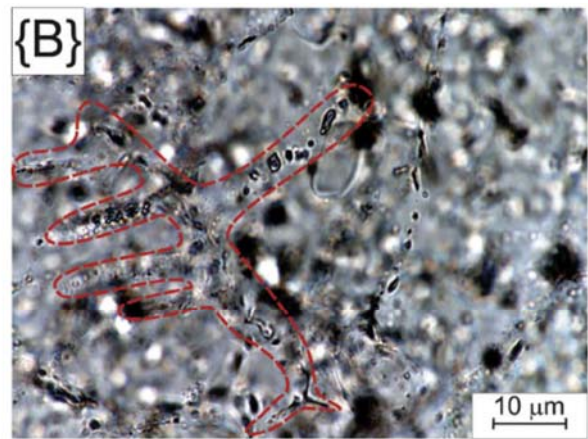
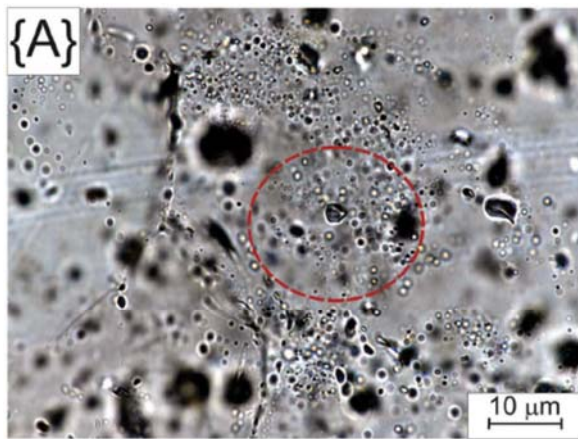


Fig. 4

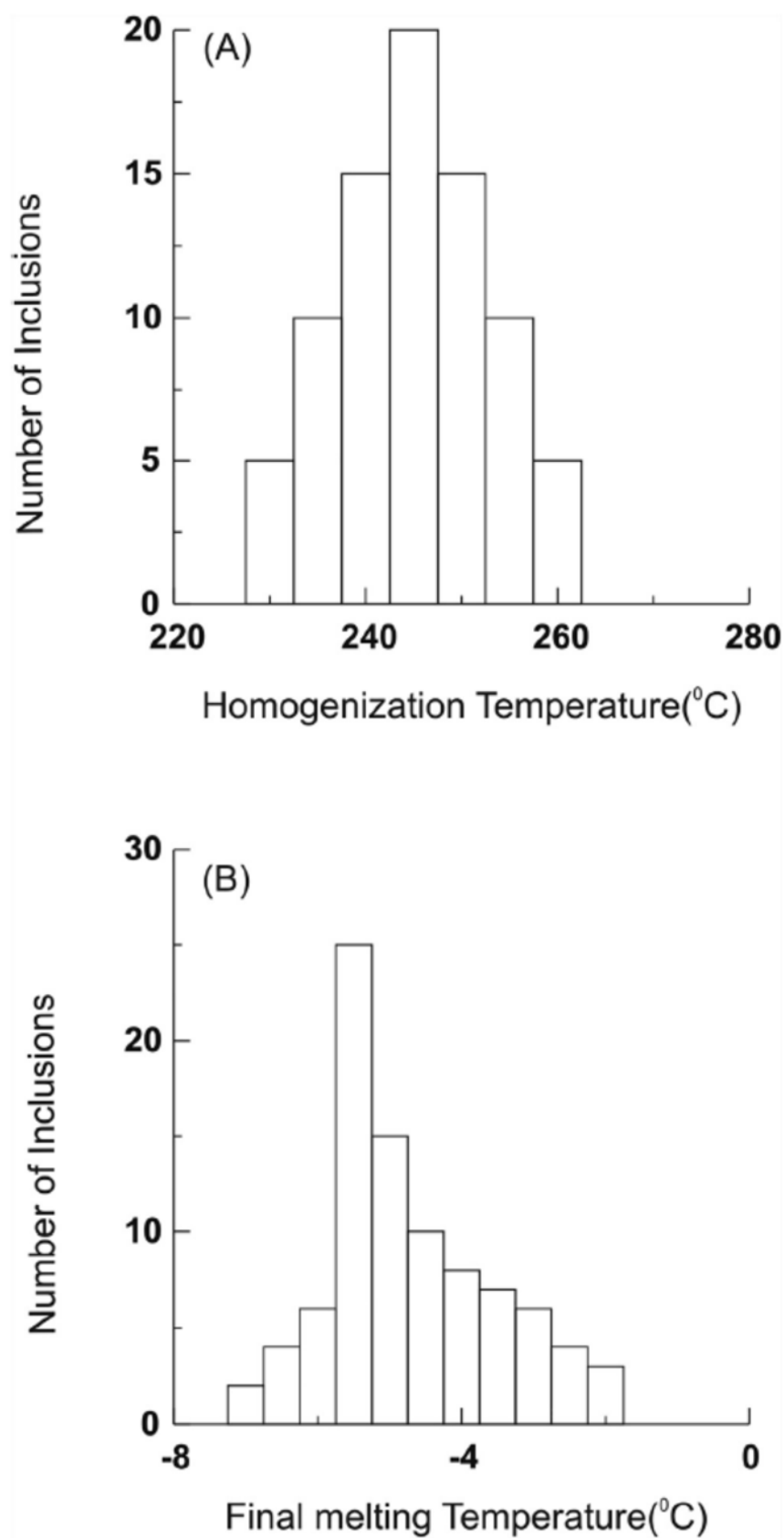


Fig. 5

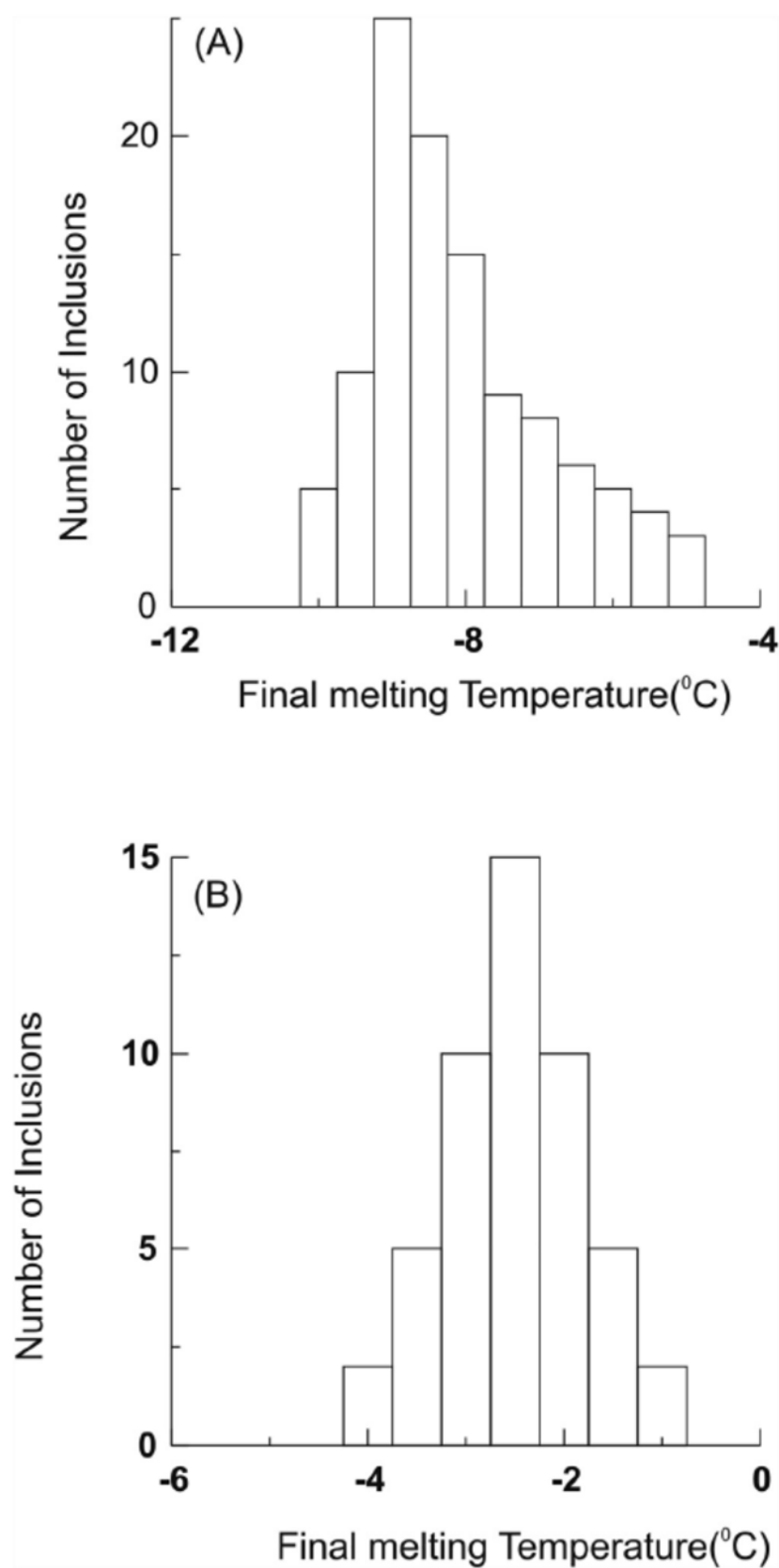
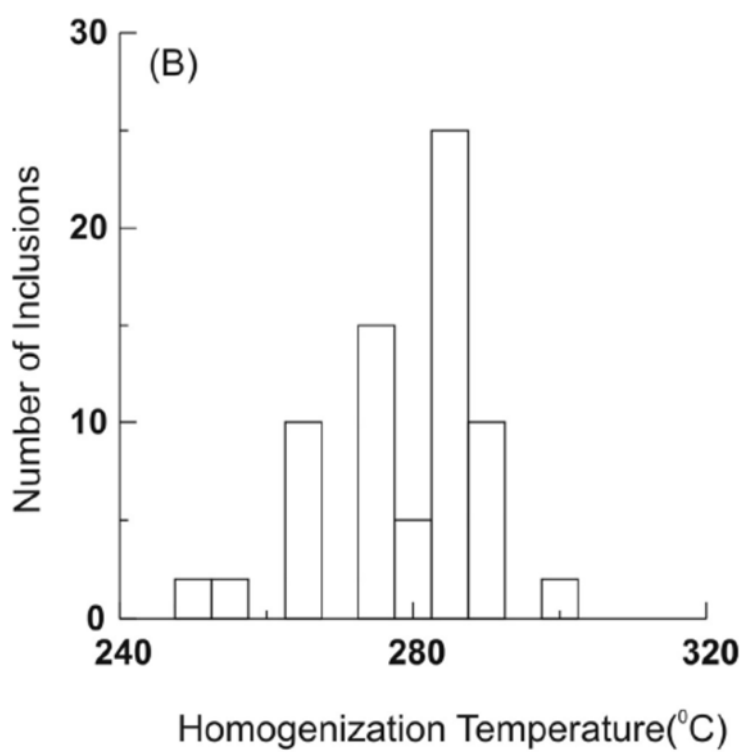
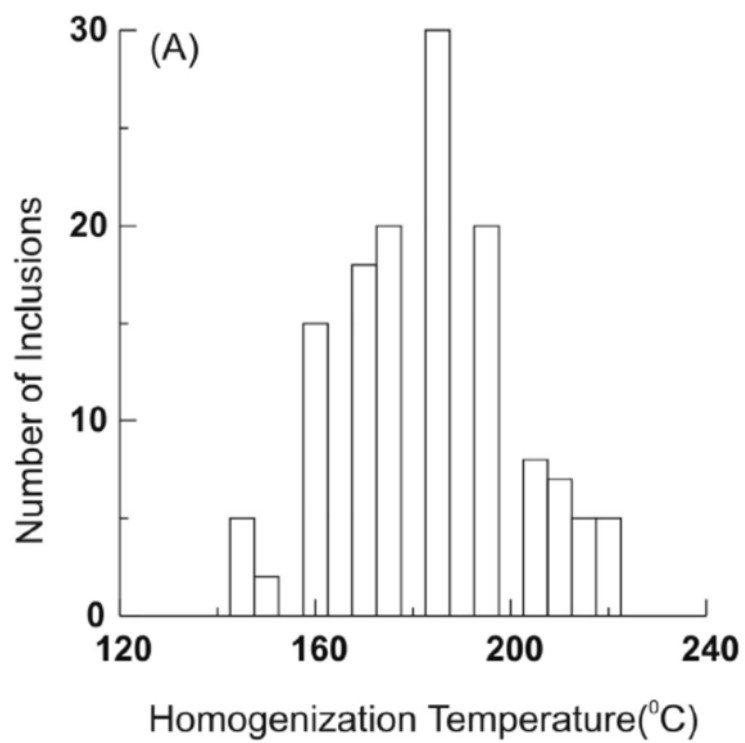


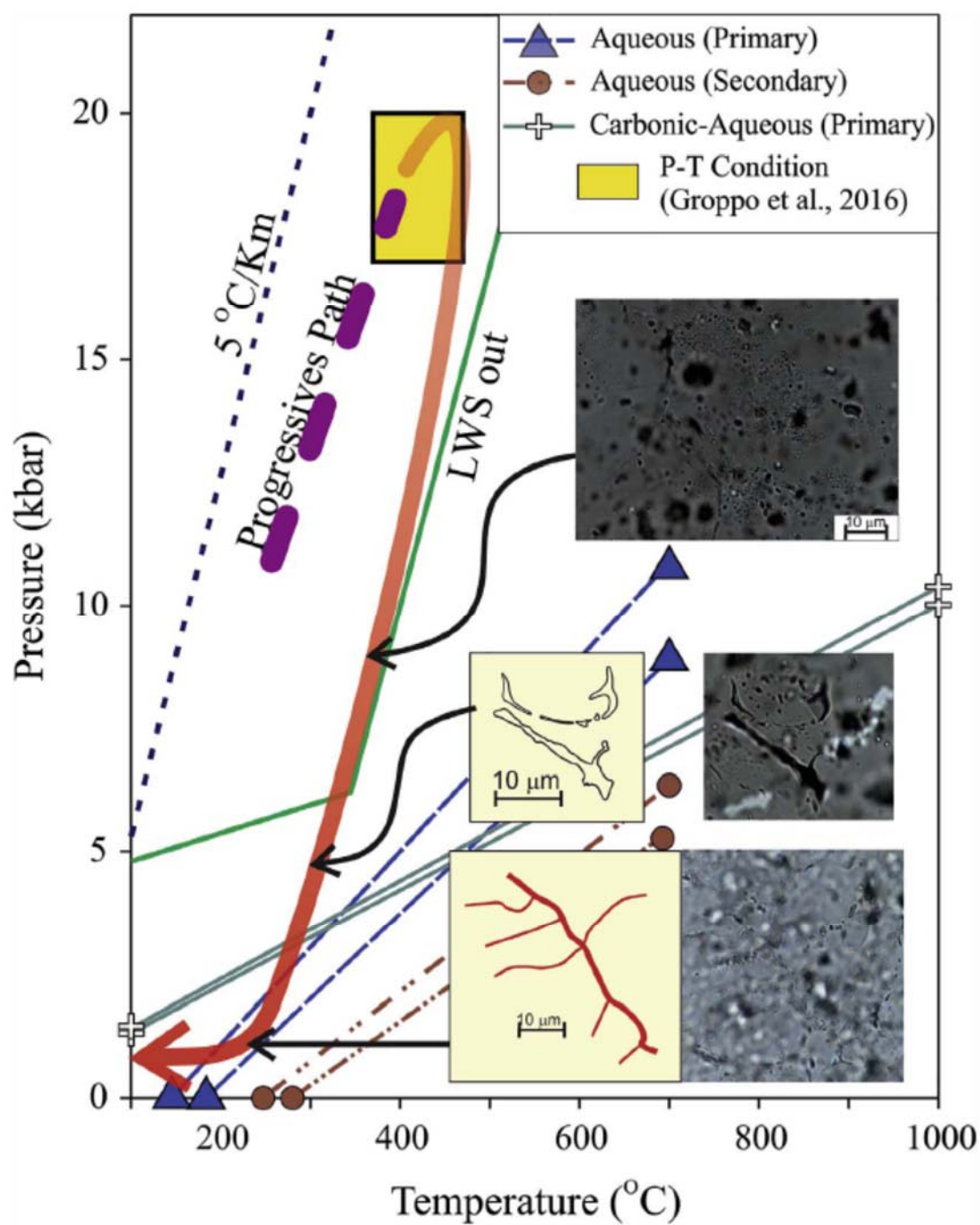
Fig. 6



628

629 Fig- 7

630



631

632 Fig.8